Int. J. Electrochem. Sci., 17 **(2022)** Article Number: 220923, doi: 10.20964/2022.09.48

International Journal of
ELECTROCHEMICAL
SCIENCE
www.electrochemsci.org

Short Communication

Surface characterization of X80 Steel and Its Aspergillus terreus induced corrosion behavior in marine environment

Hongtao Huang[1,*], *Jingyu Guo*[1], *Jiao Li*[2,*], *Liang Li*[3], *Zilong Zhao*[2,*]

[1] Sino-French Institute of Nuclear Energy and Technology, Sun Yat-Sen University, Zhuhai 519082, China;
[2] School of Chemical Engineering and Technology, Sun Yat-sen University, Zhuhai 519082, China
[3] School of Physics, Engineering and Computer Science, University of Hertfordshire, UK AL109AB
[*]E-mail: huanghongtao401@163.com, lijiao35@mail2.sysu.edu.cn, zhaozlong@mail.sysu.edu.cn

Received: 1 May 2022 / *Accepted:* 8 June 2022 / *Published:* 7 August 2022

X80 steel is an important engineering material for ship structures. The corrosion of X80 generally exists in various environments, especially in the marine environment. However, the corrosion behaviors of X80 in marine microbial Aspergillus terreus environment have not been well-addressed. In this paper, the microstructure of pipeline steel X80 was investigated by EBSD. Then, the Aspergillus terreus was added to the simulated seawater, and the electrochemical corrosion behavior of X80 was continuously tested for 21 days. The morphologies after corrosion were characterized by SEM. The products before and after corrosion were analyzed by XRD. The corrosion mechanism of pipeline steel X80 in the Aspergillus terreus concentrated environment was clarified.

Keywords: X80 steel, Microbial corrosion, Microstructure, Corrosion products, Aspergillus terreus

1. INTRODUCTION

Metals can be obtained by different methods such as smelting, electroreduction, etc. This indicates that the metal is thermodynamically unstable in nature. Therefore, there is a tendency for spontaneous corrosion, and in the process of metal corrosion, most of them belong to electrochemical corrosion. The magnitude of the electrochemical corrosion tendency can be judged by the change of Gibbs free energy. To determine whether the metal corrosion reaction can proceed.

For a long time, corrosion has been a major concern in the oil and gas industry, proving to be fatal to production in a plethora of ways, including production, exploration, transportation, infrastructure, storage, and transportation[1-4]. Corrosion not only changes the mechanical and physical properties of metal materials, but also causes major accidents, huge economic losses and pollution[5-9]. Microbial

corrosion (MIC) refers to a phenomenon in which the life activities of microorganisms in the biofilm are attached to the surface of materials (including metals and non-metals). It may cause or promote the corrosion and damage of materials. Liu et al. reported on the MIC of steel by numerous microorganisms[10-16]. In China, the annual loss due to MIC is more than 50 billion yuan[17]. According to relevant surveys, 81% of severe corrosion in the United States is related to microorganisms. At least 50% of buried metal corrosion is caused by microbial corrosion[18]. Fungus is a collective term for branching hyphae fungi. The basic unit that makes up the fungus body is called the mycelium. It has a long tubular shape with a width of 2 to 10 microns, and can continuously grow and branch from the front end. Fungus multiplies rapidly, often causing a lot of moldy spoilage of food and utensils. However, many beneficial species have been widely used, and they are the first microorganisms to be utilized and recognized in human practice.

In this paper, the microstructure of pipeline steel X80 was investigated by EBSD. Then, the fungus was added to the simulated seawater, and the electrochemical corrosion behavior of X80 was continuously tested for 21 days. The morphologies after corrosion were characterized by SEM and EDS. The products before and after corrosion were analyzed by XRD. The corrosion mechanism of pipeline steel X80 in the fungus concentrated simulated seawater environment was clarified.

3. EXPERIMENTAL PROCEDURE

The X80 steel (Baowu steel corp.) was cut into corrosion coupon with a size of 10*10*10 mm. And it had a chemical composition (wt%) of: C 0.07, Si 0.19, Mn 1.82, P 0.007, S 0.023, Mo 0.01, Ni, 0.17, Cr 0.026, Cu 0.02, Al 0.028, V 0.002, Nb 0.056, B 0.0001, N 0.004 and Fe balance. The simulated seawater was prepared by adding 3.5wt.% NaCl into deionized water. The fungus medium was added into a 200 mL simulated seawater for experiment. Aspergillus terreus (A. terreus) that isolated from the Xisha Sea area of China was used in this work, and the species of fungus was identified using polymerase chain reaction (PCR) amplification of 16S rDNA. The DNA sequence of A. terreus is as blow:

GCCAACCTCCCACCCGTGACTATTGTACCTTGTTGCTTCGGCGGGCCCGCCAGCGT
TGCTGGCCGCCGGGGGGCGACTCGCCCCCGGGCCCGTGCCCGCCGGAGACCCCAACATGA
ACCCTGTTCTGAAAGCTTGCAGTCTGAGTGTGATTCTTTGCAATCAGTTAAAACTTTCAAC
AATGGATCTCTTGGTTCCGGCATCGATGAAGAACGCAGCGAAATGCGATAACTAATGTGA
ATTGCAGAATTCAGTGAATCATCGAGTCTTTGAACGCACATTGCGCCCCCTGGTATTCCGG
GGGGCATGCCTGTCCGAGCGTCATTGCTGCCCTCAAGCCCGGCTTGTGTGTTGGGCCCTCG
TCCCCCGGCTCCCGGGGGACGGGCCCGAAAGGCAGCGGCGGCACCGCGTCCGGTCCTCG
AGCGTATGGGGCTTCGTCTTCCGCTCCGTAGGCCCGGCCGGCGCCCGCCGACGCATTTATT
TGCAACTTGTTTTTTTCCAGGTTGACCTCGGATCAGGTAGGGATACCCGCTGAACTTAAGC
ATATCTA

The open circuit potential (OCP), electrochemical impedance spectroscopy (EIS) was conducted using an electrochemical workstation (Model CS350, Corrtest, China) for the study of electrochemical corrosion process in real time. The EIS measurement was conducted after immersion in 1day, 2 days, 4

days, 7 days, 10 days, 14 days, 17 days, and 21days, respectively.

The microstructure of samples was examined by using a 3D Optical Microscopy (OM, LEICA DVM6) , a scanning electron microscope (SEM, JSM-7800 F, JEOL, Japan) equipped with an Oxford electron back-scattered diffraction (EBSD) system. Phase analysis was carried out on an XPERT-PRO X-ray diffraction (XRD) system.

3. RESULTS AND DISCUSSION

The properties of materials are determined by composition and microstructure. Even for the materials with the same composition, the mechanical properties of them with different structural orientations are quite different[19-24]. Pipeline steel is mainly used for processing and manufacturing oil and gas pipelines. In addition to high compressive strength, high low-temperature-toughness and excellent welding performance are also required. Compared with X70 pipeline steel, the yield strength of X80 pipeline steel is similar, but the tensile strength is higher than that of X70 pipeline steel. The development trend of pipeline engineering is large pipe diameter, high-pressure gas transportation, corrosive service environment, and thick-walled submarine pipelines. Therefore, modern pipeline steel should have high strength, high toughness and brittle fracture resistance, low welding carbon content and good weldability, and resistance to HIC and H_2S corrosion. From Fig. 1, the X80 grains vary from 2 to 30 microns, and the grain orientation is polycrystalline isotropic. This grain orientation is beneficial to improving the strength and plasticity of X80.

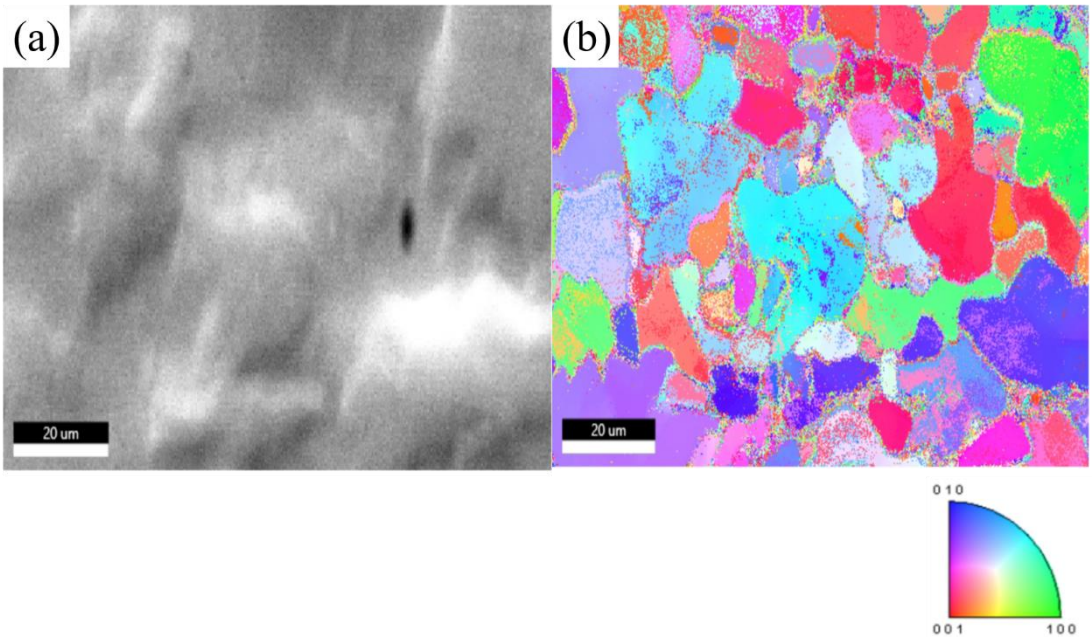

Figure 1. (a) SEM microstructure image of X80 before corrosion test, and (b) grain orientation mapping by EBSD analysis

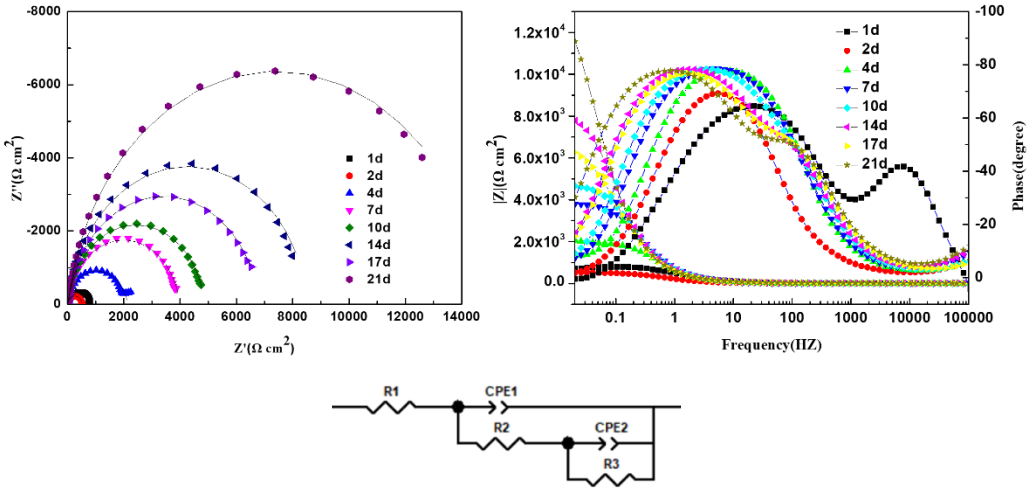

Figure 2. Time dependent of Nyquist (left) and Bode (right) plots of various specimens corresponding to different immersion times in A. terreus marine environment.

Table 1. Fitted parameters for EIS spectrum depicted in Figure 2

	R1 (Ω cm^2)	CEP1/ S*sa	CEP2/ S*sa	R2 (Ω cm^2)	R3 (Ω cm^2)
1d	1.567	4.12E-6	2.77E-4	5.623	798.6
2d	1.49	3.85E-5	7.03E-4	6.552	519
4d	2.76	4.08E-5	2.33E-4	6.114	2152
7d	4.72	5.80E-6	2.26E-4	2.268	3976
10d	6.09	1.84E-4	6.48E-5	43	4813
14d	6.99	1.87E-4	7.93E-5	74.68	8466
17d	5.96	2.12E-4	9.43E-5	81.39	6745
21d	6.98	1.88E-4	1.13E-4	103.30	14793

Fig. 2 is Electrochemical Impedance Spectroscopy (EIS) Nyquist and Bode plots of the obtained X80 steel on A. terreus. The impedance value of X80 decreased slightly in the first two days, and the corrosion rate increased. Adsorption occurred on the surface of X80 after 4 days, forming a dense protective film which slows down the corrosion rate. After 4 days, the resistance increased and the corrosion rate gradually decreased. It proves that A. terreus will adsorb on the surface of X80 to form a biological protective film, thereby slowing down the corrosion rate of pipeline steel. Liu et al. reported that the use of corrosion inhibitors and biological reagents in X80 can slow down the corrosion rate of X80, and the principle is the process of adsorption to form a protective film[25].

Fig. 3 is the morphology of X80 steel after corrosion. After MIC, there are obvious corrosion products on the surface. It is caused by the adsorption in an A. terreus corrosive environment to form biofilms. However, combined with the three-dimensional morphology of Fig. 3b, there is an unevenness of 17.15 μm after 21 days of corrosion, indicating that the formed biofilm is micron scale. As the corrosion progresses for a long time, the active sites on the alloy surface will break down the protective film and localized corrosion will occur[25, 26].

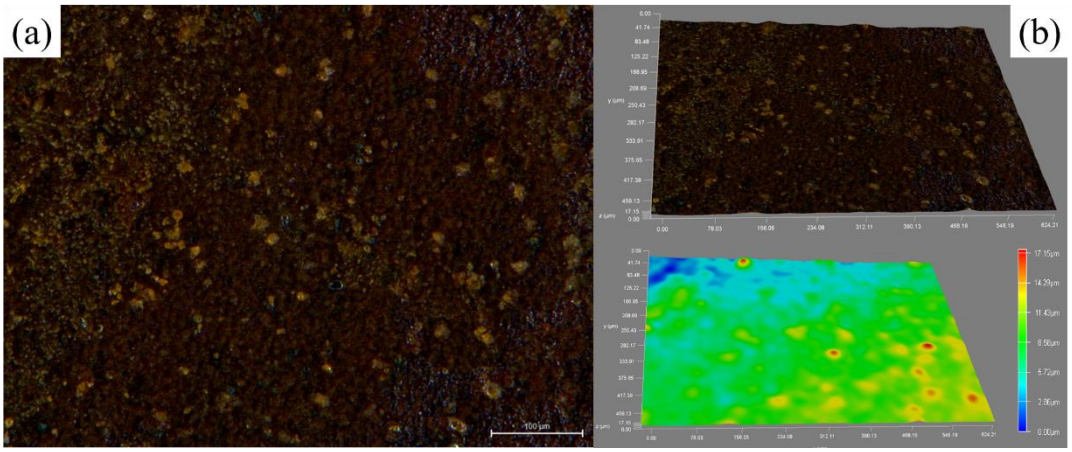

Figure 3. 3D OM images of X80 steel after corrosion

It indicates that microbial corrosion is a long-term and complex process. Generally, microorganisms first attach to the hull surface and then release acidic metabolites to accelerate corrosion. Metabolite-formed mucous membranes constitute large-area electrochemical corrosion cells to further accelerate alloy corrosion[4, 27-30]. From Fig. 4a, the surface of X80 steel after corrosion is smooth and there is no obvious localized corrosion after the biofilm is removed by vibration polishing. At the high magnification (Fig. 4b), there are tiny nano-etched pits on the surface. Such tiny nano-corrosion pits are not enough to reduce the corrosion resistance of X80 pipeline steel after 21 days of corrosion in an A. terreus environment. There are also micron-scale corrosion areas, but no large corrosion pits are formed. The corrosion damage of A. terreus to X80 pipeline steel is far less than that of SRB. On the contrary, A. terreus can form a certain biological protective film to slow down the corrosion of X80 pipeline steel.

Fig. 5 is XRD (X-Ray Diffraction) pattern of X80 steel before and after corrosion. There is no obvious change in the product before and after corrosion. The peak at 14 degree is enhanced after corrosion, indicating that the biofilm formed by corrosion products in the A. terreus corrosion environment is amorphous.

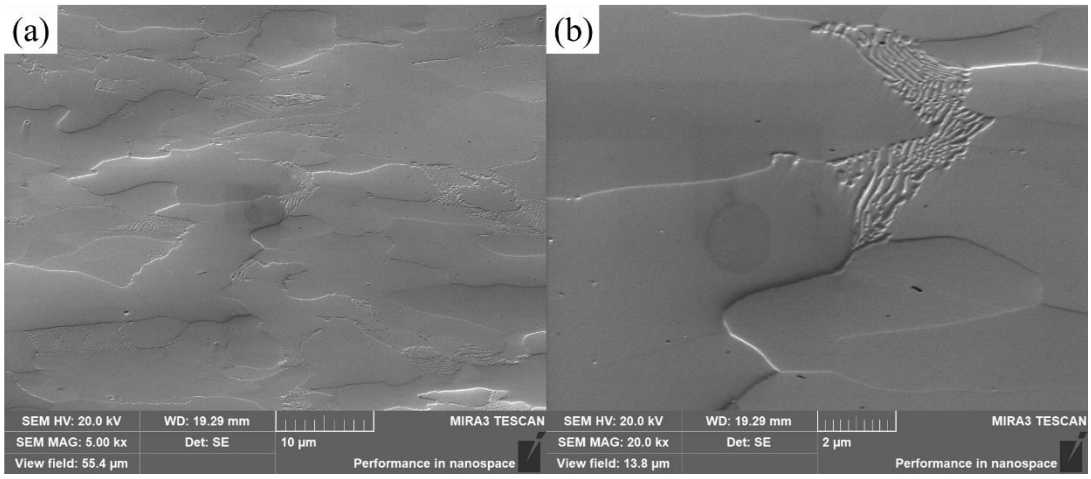

Figure 4. SEM images of X80 steel after corrosion. Low magnification (a) and high magnification (b).

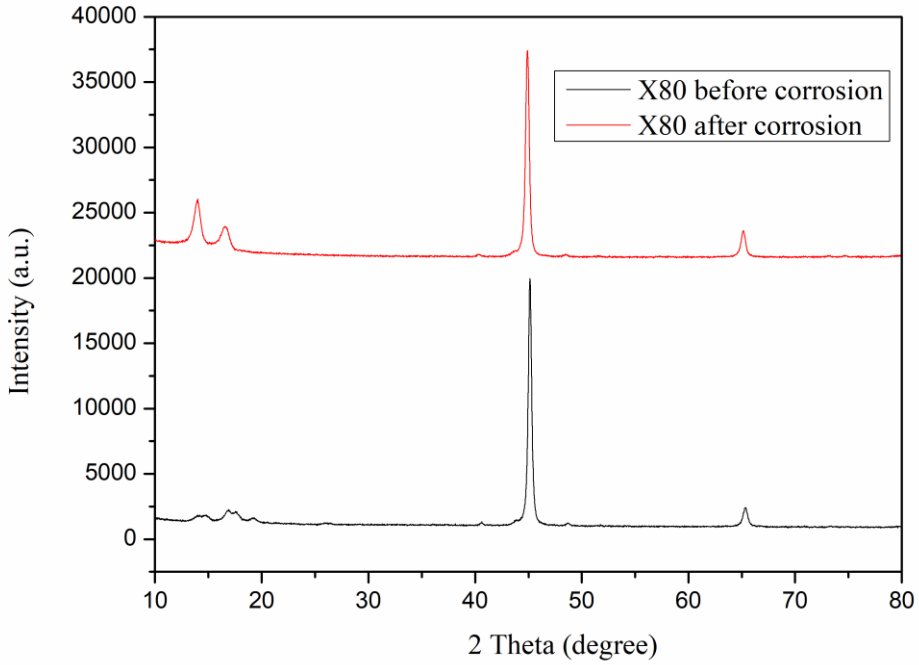

Figure 5. XRD (X-Ray Diffraction) pattern of X80 steel before and after corrosion test

4. CONCLUSION

1. the X80 grains vary from 2 to 30 microns, and the grain orientation is polycrystalline isotropic. This grain orientation is beneficial to improving the strength and plasticity of X80.

2. The EIS low frequency impedance value of X80 decreased slightly in the first two days, and the corrosion rate increased. However, adsorption occurred on the surface of X80 after 4 days, forming a dense protective film. This slows down the corrosion rate. After 4 days, the resistance increased and the corrosion rate gradually decreased. It shows that A. terreus will adsorb on the surface of X80 to form a biological protective film, thereby slowing down the corrosion rate of pipeline steel.

3. After the corrosion test, the surface of X80 steel is smooth with only tiny nano pits. Such tiny nano-corrosion pits were not enough to reduce the corrosion resistance of X80 pipeline steel after 21 days of corrosion in an A. terreus environment.

ACKNOWLEDGEMENTS
The authors gratefully acknowledge the financial support from the National Natural Science Foundation of China (NSFC) (No. 51903253) and the Natural Science Foundation of Guangdong Province of China (2019A1515011150).

References

1. V. B. Sharma, K. Singh, R. Gupta, A. Joshi, R. Dubey, V. Gupta, S. Bharadwaj, M. I. Zafar, S. Bajpai, M. A. Khan, A. Srivastava, D. Pathak and S. Biswas, *Applied System Innovation*, 4 (2021) 14-18.
2. Z. Y. Feng, B. Hurley, M. L. Zhu, Z. Yang, J. Hwang and R. Buchheit, *J Electrochem Soc*, 166,

C520 (2019) 28-32.
3. S. Chen, Z. Huang, M. Yuan, G. Huang, H. Guo, G. Meng, Z. Feng and P. Zhang, *J Mater Sci Technol*, 67 (2022) 125.
4. Z. Feng, J. Li, J. Ma, Y. Su, X. Zheng, Y. Mao and Z. Zhao, *Journal of Marine Science and Engineering*, 10 (2022) 23-25.
5. L. Stemper, M. A. Tunes, P. Dumitraschkewitz, F. Mendez-Martin, R. Tosone, D. Marchand, W. A. Curtin, P. J. Uggowitzer and S. Pogatscher, *Acta Materialia*, 206 (2021) 81-83.
6. R. Arrabal, B. Mingo, A. Pardo, M. Mohedano, E. Matykina and I. Rodriguez, *Corrosion Science*, 73 (2013) 342.
7. Y. Y. Wang, Y. J. Luo, H. Xu and H. J. Xiao, *Journal of Central South University*, 27 (2020) 1224.
8. Z. Y. Feng, B. Hurley, J. C. Li and R. Buchheit, *J Electrochem Soc*, C94 (2018) 165.
9. Z. Feng, C. C. Xu, D. Zhang and R. Buchheit, *Materials*, 14 (2021) 286.
10. H. Liu and Y. F. Cheng, *Corrosion Science*, 173 (2020) 96-98.
11. H. Liu and Y. F. Cheng, *Journal of Materials Research and Technology-Jmr&T*, 9 (2020) 7180.
12. H. Liu, Y. Zhang, W. Li, G. Meng, W. Zhang and H. Liu, *Industrial & Engineering Chemistry Research*, 58 (2019) 17668.
13. H. Liu, T. Gu, G. Zhang, H. Liu and Y. F. Cheng, *Corrosion Science*, 47 (2018) 136.
14. H. Liu, M. Sharma, J. Wang, Y. F. Cheng and H. Liu, *International Biodeterioration & Biodegradation*, 129 (2018) 209.
15. H. Liu and Y. F. Cheng, *Electrochimica Acta*, 266 (2018) 312.
16. H. Liu and Y. F. Cheng, *Electrochimica Acta*, 253 (2017) 368.
17. X. Shi, C. Yang, W. Yan, D. Xu, M. Yan, Y. Shan and K. Yang, *Journal of Chinese Society for Corrosion and Protection*, 39 (2019) 9.
18. Y. Lou, W. Chang, T. Cui, J. Wang, H. Qian, L. Ma, X. Hao and D. Zhang, *Bioelectrochemistry*, 141 (2021) 11-12.
19. Z. Zhao, Z. Sun, W. Liang, Y. Wang and L. Bian, *Materials Science and Engineering a-Structural Materials Properties Microstructure and Processing*, 702 (2017) 206.
20. Z. Zhao, B. Duan, J. Ying and L. Li, *Jom*, 73 (2021) 2558.
21. Z. Zhao, J. Chen, X. Wu and F. Liu, *Materials Today Communications*, 27 (2021) 32370.
22. Z. Y. Feng, J. C. Li, Z. Yang and R. Buchheit, *Materials*, 13 (2020) 45-47.
23. Z. Zhao, X. Jiang, S. Li, L. Li, Z. Feng and H. Lai, *Crystals*, 12 (2022) 49-52.
24. Z. Zhao, X. Liu, S. Li, Y. Mao, Z. Feng, W. Ke and F. Liu, *Jom-Us* (2022) 8-11.
25. H. Liu, C. Chen, X. Yuan, Y. Tan, G. Meng, H. Liu and Y. F. Cheng, *Corrosion Science*, 203 (2022) 110345.
26. Y. Zhang, J. He, L. Zheng, Z. Jin, H. Liu, L. Liu, Z. Gao, G. Meng, H. Liu and H. Liu, *Npj Mat Degrad*, 6 (2022) 27.
27. Z. Zhao, Y. Li, Y. Zhong and Y. Liu, *International Journal of Electrochemical Science*, 14 (2019) 6394.
28. Z. Zhao, Y. Liu, Y. Zhong, X. Chen and Z. Zhang, *International Journal of Electrochemical Science*, 13 (2018) 4338.
29. X. Zheng, H. S. Lai and Z. Zhao, *International Journal of Electrochemical Science*, 16 (2021) 63-65.
30. G. Zhang, L. Wu, A. Tang, S. Zhang, B. Yuan, Z. Zheng and F. Pan, *Advanced Materials Interfaces*, 4 (2017) 105-108.